Pergamon

Atmospheric Environment Vol. 30, No. 24, pp. 4197–4207, 1996

PII: S1352-2310(96)00144-6
1352-2310/96 $15.00 + 0.00

A LAGRANGIAN DISPERSION MODEL FOR CALCULATING CONCENTRATION DISTRIBUTION WITHIN A BUILT-UP DOMAIN

H. KAPLAN and N. DINAR
Israel Institute for Biological Research, P.O.B. 19 Ness-Ziona, Israel

(*First received* 8 *August* 1995 *and in final form* 25 *April* 1996)

Abstract—A Lagrangian model to study the dispersion of pollutants between urban buildings is described. The flow field is supplied by an objective analysis (Rockle (1990) Ph.D. thesis, Vom Fachbereich Mechanik, der Technischen Hochschule Darmstadt, Germany) and is adjusted to satisfy the continuity equation. From the resulting mass consistent field the Lagrangian diffusion parameters are eliminated. A 3-D Lagrangian diffusion model in a nonhomogeneous field is applied to calculate the pollutant distribution between the buildings. Several examples are studied and compared to wind tunnel measurements. Copyright © 1996 Elsevier Science Ltd

Key word index: Built-up area, mass consistent field, Lagrangian diffusion, diagnostic models, buildings, concentration fields.

1. INTRODUCTION

The dispersion of toxic gases resulting from an accidental release within an urban area is a subject for many investigations. In the near-field region of the source when most of the material is between the buildings, the dispersion is site dependent and is influenced by the structure of the buildings and the complex vortex system in the streets. Later, when the vertical size of the plume is larger than the average height of the buildings, the dispersion is influenced by the atmospheric properties above the urban area and the influence of the buildings is reflected as parameters of the dispersion constants and the wind profiles in the boundary layer. In most urban dispersion studies, which were directed to air pollution problems, the near-field influence of the buildings was neglected and the Gaussian model was used with modified standard deviations (see e.g. Hanna and Chang, 1992; Briggs, 1973). Other studies take into account the influence of the near field, by modifying the diffusion constants in the region where the vertical spread, σ_z, is of the order of the average building height (Bowne, 1974). There are models which describe the dispersion within specific urban structure like an urban street canyon (Yamartino and Wiegard, 1986).

In the general case the interaction of different types of urban structures causes several phenomena that are not described by the simple Gaussian models but may affect the hazard zone. Such phenomena are, for example

(1) upwind dispersion (Rockle, 1994),

(2) shift of the plume center as a result of the flow channelling in the streets (Cermak and Takeda, 1985),

(3) appearance of high or low concentrations at specific points (Beachlin *et al.*, 1992),

(4) nonmonotonic behavior of the vertical concentration profile within the street level. For example higher concentrations can be observed at levels above the ground even for ground-level sources (Rockle, 1994).

All those phenomena can significantly affect decision making and monitoring procedures. It is therefore important to develop models for describing the dispersion in the near field of the source.

There is a considerable amount of work on dispersion in complex terrain (see e.g. Hunt (1985)). The main difficulty in adapting these techniques to describe the diffusion in a built-up area is in modelling the turbulent fluxes. The reason is that in a built-up area when the streamlines are close to the obstacles and there are steep gradients in the boundaries of the flow, the turbulence is weakly correlated with the upwind turbulence. Prognostic models that solve the Navier–Stokes equations were used to describe the flow around an isolated building (Zhang *et al.*, 1993) or the interaction of two buildings (Lee, 1992). Those models used the K–ε approach to describe the turbulent flow. Eichhorn *et al.* (1988) describes the urban phenomena by a nonhydrostatic prognostic model, in which the equations were closed using the K-gradient approach. All those models require free stream boundary conditions. It is therefore impractical to use them to describe the flow within a small domain inside a large city. It is also very difficult to

apply prognostic models to describe the flow over a domain of the size of the whole city. Such a domain which is of order of 10×10 km requires matrices of huge size in order to resolve the vortex structure at street level, where a resolution of 5 m or less is needed, both vertically and horizontally.

In order to overcome this problem Rockle (1990) suggested a diagnostic model for flow around building clusters. In this approach the initial field is supplied by objective analysis. Then this field is adjusted to satisfy the continuity equation using a least squares variational technique which was suggested by Sherman (1978).

In this work we adopt the approach of Rockle for the initial field. Then a mass consistent adjusted field is obtained using a fast multigrid numerical algorithm. From this mass consistent field we eliminate the Lagrangian parameters: σ_V, the turbulent velocity, and T_L, the Lagrangian time scale. These parameters are used in a Lagrangian diffusion model to calculate concentrations from a continuous source at the street level.

In the following we describe in detail the stages of this approach: In Section 2 a brief description of the initial field suggested by Rockle (1990) is described. In Section 3 we describe the mass consistent procedure. Section 4 will describe the Lagrangian model and the elimination of the diffusion parameters. In Section 5 several examples are studied. In all those examples the model is applied to clusters of a few buildings in order to compare the results with other calculations. However, the model is capable and was applied successfully to a subdomain of a real city of order 1×1 km. Those results will be described in another paper. The results of the present calculations are discussed and summarized in Section 6.

2. THE INITIAL FIELD

The initial field is determined as suggested by Rockle in his Ph.D thesis (Rockle, 1990). We shall give here a brief description of his procedure:

2.1. *Flow near an isolated obstacle*

2.1.1. *Wind normal to the obstacle.* An isolated obstacle is characterized by its height H, alongwind length L and width W. Three regions characterize the flow in the neighborhood of the building (Fig. 1):

(1) displacement zone in its upwind side,
(2) cavity zone in its lee side,
(3) wake zone downwind to the cavity zone.

A "displacement zone" is established on the upwind side of the building, when boundary layer wind is incident normally on such obstacle. A standing eddy is present in this zone and the main flow is separated from the ground and reattached at the wall at a height of about $0.6H$. The distance of the "displacement zone", L_F, depends on the obstacle dimensions and is given by (Hosker, 1984):

$$\frac{L_F}{H} = \frac{2(W/H)}{1 + 0.8\,W/H}. \tag{1}$$

Rockle suggests describing this zone by the volume bounded by the surface:

$$\frac{X^2}{L_F^2(1 - (Z/0.6H)^2)} + \frac{Y^2}{W^2} = 1 \tag{2}$$

where X, Y, Z are alongwind, crosswind and height coordinates, respectively. In this zone the average wind is zero.

Separation of flow occurs also on the downwind side of the obstacle. This zone is called the "cavity zone". The flow in this zone is very complex. The alongwind extension of the cavity zone, L_R (after Hosker (1984) is given by

$$\frac{L_R}{H} = \frac{1.8\,W/H}{(L/H)^{0.3}(1 + 0.24\,W/H)}. \tag{3}$$

The main flow pattern in the "cavity zone" is the lee-edge vortex which exhibits near ground flow in the opposite direction to the wind on the roof level, $U(H)$. The "cavity zone" is described by the volume bounded

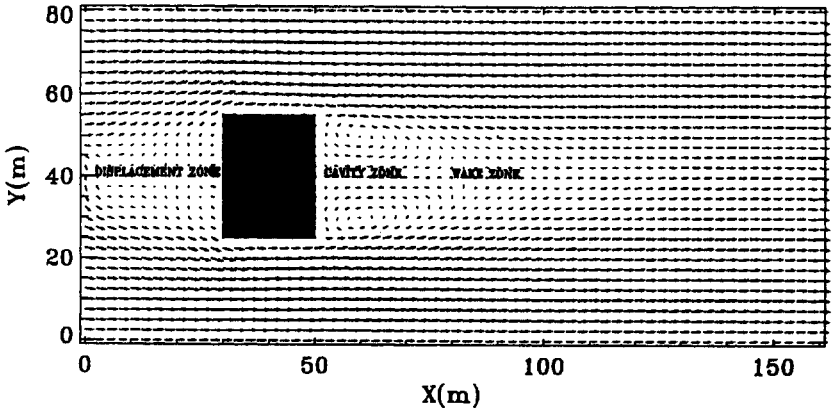

Fig. 1. The flow zones near a rectangular obstacle.

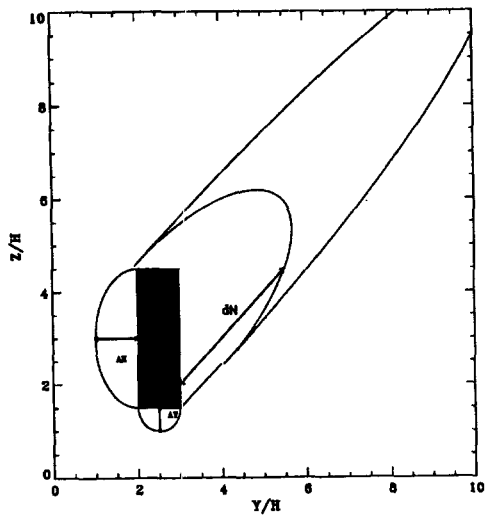

Fig. 2. Flow zones for flow at an angle to the obstacle.

by the surface:

$$\frac{X^2}{L_R^2(1-(Z/H)^2)}+\frac{Y^2}{W^2}=1. \tag{4}$$

The wind in this zone is in opposite direction to the roof level wind and decays to zero on the surface of the zone:

$$U=U(H)\left(1-\frac{X}{d_N}\right)^2 \tag{5}$$

where d_N is the downwind extension of the zone through the point location (Fig. 2).

$$d_N=L_R\sqrt{\left(1-\left(\frac{Z}{H}\right)^2\right)\left(1-\left(\frac{Y}{W}\right)^2\right)}-0.5L. \tag{6}$$

Downwind to the "cavity zone" a turbulent layer develops above the ground. This zone is called the "wake zone". Within the wake zone there is a difference between the velocity wind profile observed at the point location with and without the obstacle. This difference is called the "velocity defect" and decays to zero like $(X/H)^{1.5}$. The distance of the extension of the wake zone is about three times that of the cavity zone. Rockle suggests describing the wind in this zone by

$$U(Z)\left(1-\left(\frac{d_N}{X}\right)^{1.5}\right) \tag{7}$$

where $U(Z)$ is the boundary layer wind profile in absence of obstacles.

2.1.2. *Wind at an angle to the obstacle.* When the angle Θ between the wind direction and the building orientation is not zero this simple description of the flow field is modified in the following way: Two displacement zones are established on the two building's upwind side (see Fig. 2).

The volume of each zone is bounded by the surface:

$$\left(\frac{X}{A_X}\right)^2+\left(\frac{Y}{A_Y}\right)^2=1 \tag{8}$$

where A_X, A_Y, and the wind in each zone are described in Table 1.

In order to describe the cavity and wake zones one defines an effective width W_{eff} and length L_{eff} of the building as the projection of the obstacle dimensions pependicular and parallel to the wind direction, respectively. L_F is determined by formula 1 with W_{eff}, L_{eff}, instead of W and L, respectively. The cavity zone and wake zone are described by equation (8) with the parameters A_x and A_y presented in Table 2. In Table 2 d_l is the distance of the point at which the wind profile is calculated from the obstacle.

2.2. *Flow near array of obstacles*

The flow in the near field of an array of obstacles was investigated by many authors and a review is given by Hosker (1984). This flow depends on the density of the obstacles. When the obstacles are placed well apart one can treat the flow field as the sum of the flow of the isolated obstacles. This regime is called by Rockle regime I. When the obstacles are placed closer, their individual flow fields interact and are disturbed. This regime is called regime II. When obstacles are close enough, stable vortices are produced in the gaps between the elements and the main flow no longer penetrates into those gaps but skims over the array top. This region which is denoted as regime III, was investigated intensively in the literature and is called also the canyon flow (see e.g. Holzworth, 1972; Hotchkiss and Harlow, 1973; Yamartino and Wiegard, 1986; Hunter *et al.*, 1992). One of the parameters that characterize those three regions is the face to face space, S. The transition from regime I (isolated obstacles) to regime II (interim regime) occurs for $S < S^*$ where S^* is given by

$$\frac{S^*}{H}=1+1.4\left(\frac{W}{H}\right)^{0.5} \quad 0.5\leqslant\frac{W}{H}\leqslant 4. \tag{9}$$

Table 1. Wind flow in the displacement zone

	X-direction zone	Y-direction zone
A_X	$L_F\sin^2\Theta\sqrt{1-(Z/0.6H)^2}$	$0.5L$
A_Y	$0.5W$	$L_F\cos^2\Theta\sqrt{1-(Z/0.6H))^2}$
Wind velocity	$U=0$	$V=0$

Table 2. Wind flow in the cavity and wake zone

Zone	Cavity	Wake
A_x	$L_R\sqrt{1-(Z/H)^2}$	$3L_R\sqrt{1-(Z/H)^2}$
A_Y	$0.5W_{eff}$	$0.5W_{eff}$
Wind Velocity	$U = -U(H)(1-d_l/d_N)^2$ $V = -V(H)(1-d_l/d_N)^2$	$U = U(Z)(1-d_N/d_l)^{1.5}$ $V = V(Z)(1-d_N/d_l)^{1.5}$

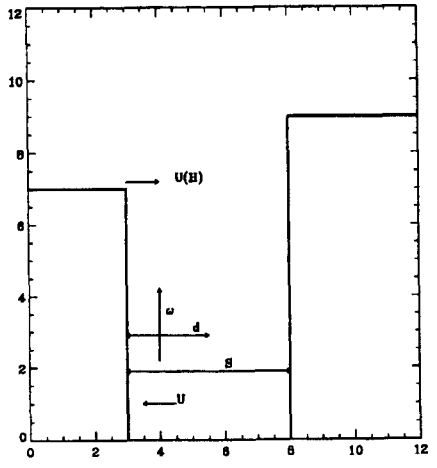

Fig. 3. Standing vortex in the street canyon.

The transition to the skimming flow (regime III) occurs for $S < S^{**}$ where S^{**} is given by

$$\frac{S^{**}}{H} = \begin{cases} 1.25 + 0.15W/H & W/H < 2, \\ 1.55 & W/H \geqslant 2. \end{cases} \tag{10}$$

2.2.1. *The initial wind field in the skimming flow regime.* If the undisturbed flow is normal to the obstacle's surface, the initial field for a standing vortex within the street canyon is

$$U = -U(H)d/0.55(S - d/0.5S)$$
$$\omega = \left|\frac{U(H)}{2}\left(1 - \frac{d}{0.5S}\right)\right|\left(1 - \frac{S-d}{0.5S}\right) \tag{11}$$

where $U(H)$ is the wind velocity at the upwind obstacle's top, d is the distance of the point from the upwind obstacle's face, S is the canyon width, U is the cross wind component of the wind and ω its vertical component inside the street canyon (see Fig. 3). If the angle between the street direction and the wind flow is not zero we decompose the wind into $U_{||}$ and $U_{\perp}$, components parallel and perpendicular to the street direction, respectively. The parallel component remains unchanged:

$$U_{||} = U_{||}(Z) \tag{12}$$

The perpendicular component $U_{\perp}$ creates the standing vortex and is substituted in equation (11) instead of U.

Points that are located in regime II belong to regime I or regime III according to the following criteria: Let N be the number of grid points found on a line through the point in the street direction within $\pm$ 25 m from the point. Let M be the number of points out of N for which the width of the street, S, through them is less than 30 m. If $M/N > 0.5$, the grid point is attributed to region III otherwise it is attributed to region I.

2.2.2. *Flow field above the obstacle's top.* The flow field above the obstacle's top is described by the logarithmic profile with the zero plane displacement, D, and the roughness length Z_0 (Hanna, 1992).

$$U(Z) = \frac{U_*}{k}\ln\frac{Z-D}{Z_0} \tag{13}$$

k is the von Karman constant and U_* the friction velocity.

Following Rockle (1990), the zero plane displacement is given by

$$D = 0.8\frac{\sum_i W_i L_i H_i}{\sum_i W_i L_i} \tag{14}$$

and the roughness length

$$Z_0 = 0.2\frac{\sum_i W_i L_i H_i}{\sum_i L_X L_Y} \tag{15}$$

where L_X, L_Y are the domain dimensions.

3. THE MASS CONSISTENT PROCEDURE

The initial diagnostic field described in the previous section, redefined here as $\mathbf{U}_0 = (u_0, v_0, w_0)$, does not satisfy the continuity equation, i.e.

$$\nabla\mathbf{U}_0 \neq 0. \tag{16}$$

The goal of the following procedure is to define a new corrected field, $\mathbf{U} = (u, v, w)$, which satisfies the following conditions:

(1) $\mathbf{U}$ satisfies the continuity equation, i.e. it is mass consistent,

(2) $\mathbf{U}$ is as close as possible to the initial field $\mathbf{U}_0$.

A procedure to force the field to satisfy the continuity equation was suggested first by Sherman (1978) and a review paper is given by Ratto (1994). The main innovations of our numerical procedure described below are:

- a very fast algorithm which allows the solution of the problem efficiently even in modest computers,
- an easy and convenient way to treat the complex irregular boundaries due to the presence of buildings.

A mass consistent wind field may be obtained by solving the variational problem of minimizing the following functional:

$$I(u, v, w) = \iiint_V [\alpha_1(u-u_0)^2 + \alpha_2(v-v_0)^2 + \alpha_3(w-w_0)^2 + \lambda\nabla\mathbf{U}]\,dx\,dy\,dz \tag{17}$$

where V is the 3-D region of interest. $\lambda = \lambda(x, y, z)$ is a Lagrange multiplier function and α_i, $i = 1, 2, 3$, are positive weights. α_i may be taken as coordinate dependent, but in most calculations they are taken as constants. The role of α is to enhance or restrict the correction of the wind components with respect to each other. The Euler equations derived from equation (17) are

$$u = u_0 + \frac{1}{2\alpha_1}\frac{\partial \lambda}{\partial x}$$

$$v = v_0 + \frac{1}{2\alpha_2}\frac{\partial \lambda}{\partial y} \tag{18}$$

$$w = w_0 + \frac{1}{2\alpha_3}\frac{\partial \lambda}{\partial z}$$

which together with

$$\frac{\partial u}{\partial x} + \frac{\partial v}{\partial y} + \frac{\partial w}{\partial z} = 0 \tag{19}$$

compose a system of four equations with four unknowns u, v, w, λ. By taking the divergence of equation (18) and applying equation (19), we obtain an elliptic equation for the Lagrange multiplier function, λ:

$$\frac{\partial}{\partial x}\left(w_1\frac{\partial \lambda}{\partial x}\right) + \frac{\partial}{\partial y}\left(w_2\frac{\partial \lambda}{\partial y}\right) + \frac{\partial}{\partial z}\left(w_3\frac{\partial \lambda}{\partial z}\right) = -\nabla\cdot\mathbf{U}_0 \tag{20}$$

where $w_i = 1/\alpha_i$. The boundary conditions are $\lambda = 0$ on open or "flow through" boundaries and $\partial\lambda/\partial n = 0$ on solid boundaries (see Ratto, 1994). In the presence of buildings the discretization of the problem to a finite difference numerical scheme becomes very complex. The first reason is that very high resolution is required for resolving all the flow features among the buildings. The second reason is the irregular solid boundaries which require complex formulation and programming for the boundary conditions. In order to overcome these difficulties a new approach for solving equation (20) is suggested:

- The equation is solved in a *regular* domain which includes the buildings.

The initial field is defined on a discrete 3-D homogeneous field as described in the previous section. The initial field is defined as zero inside the buildings and on their boundaries.

- A fast multigrid algorithm (Dinar, 1984) is applied to solve equation (20).
- During the procedure the windfield $\mathbf{U}$ is constrained to remain zero inside the buildings and on their boundaries. Equation (20) is solved several times and the procedure is stopped when the norm of the divergence of U becomes smaller than a given value.

The above algorithm is very fast. A typical problem on a domain of dimensions of order $(10^2 \times 10^2 \times 10^1)$ and resolution of 2.5–5 m requires only few minutes on a 550 RS6000 IBM workstation.

In the above procedure the weights w_i were taken as constants. A better convergence can be achieved if w_i are made coordinate dependent. This is important because of the large gradients which develop near the boundaries of the buildings. An extension of the procedure for coordinate dependent weights is now in progress. Another benefit that is gained by this extension is that different grids are possible for the different coordinates. This is important because in most applications higher resolution is required in the vertical direction than in the horizontal one. This is not possible in the present procedure.

4. THE LAGRANGIAN DIFFUSION MODEL

In the following we describe a Lagrangian diffusion model for passive scalars. In this model we assign to the contaminant particle the velocity of the fluid in its location and neglect its own inertiality. In the Lagrangian diffusion model frame, the motion of a fluid particle is described by the stochastic equations (Kaplan and Dinar, 1993):

$$\frac{d\mathbf{r}}{dt} = \mathbf{v}(\mathbf{r}, t) + \mathbf{U}(\mathbf{r}, t)$$
$$\mathbf{u}(\mathbf{r}, t) = \mathbf{a}(\mathbf{r}, t)dt + \mathbf{b}(\mathbf{r}, t). \tag{21}$$

In these equations $\mathbf{r}$ is the particle location, $\mathbf{U}(\mathbf{r}, t)$ and $\mathbf{v}(\mathbf{r}, t)$ are the average field velocity and the turbulent velocity components, respectively, at the particle location. The particle's acceleration is composed of two parts: a random part and a deterministic part. The random part, $b^\alpha(\mathbf{r}, t)$ is given by

$$b^\alpha(\mathbf{r}, t) = \sigma_v^\alpha(\mathbf{r})\sqrt{\frac{dt}{T_L^\alpha(\mathbf{r})}}\xi \quad \alpha = x, y, z \tag{22}$$

$\sigma_v(\mathbf{r})$—the turbulent velocity standard deviation and $T_L(\mathbf{r})$—the Lagrangian time scale at the particle's location. ξ is a white noise random number. The deterministic part of the acceleration is a sum of two terms:

$$a^\alpha(\mathbf{r}, t) = -\frac{v^\alpha(\mathbf{r}, t)}{T_L^\alpha(\mathbf{r})} + 0.5\frac{\partial(\sigma_v^\alpha(\mathbf{r})^2)}{\partial r^\alpha}\left(1 + \left(\frac{v^\alpha}{\sigma_v^\alpha(\mathbf{r})}\right)^2\right). \tag{23}$$

The first term is the velocity correlation term. The second term is the drift velocity which should be added to the equation in cases when σ_v is r-dependent. This term is required for satisfying the well-mixed principle (Thomson, 1987).

The parameters for the Lagrangian model $\sigma_v(\mathbf{r})$ and $T_L(\mathbf{r})$ are derived from the average wind velocity in the following way:

The Lagrangian time scale in case of neutral flow is given by $(dU/dZ)^{-1}$. Since in the presence of obstacles there is no preferred direction for the wind shear, we assume isotropy and this relation can be extended by

$$T_L = 1/|\nabla \times \mathbf{U}|. \tag{24}$$

The Eulerian correlation length in the neutral case is Z, due to the attached ground eddies whose scale is limited by their distance from the ground (Townsend, 1956). In the presence of buildings we assume that this scale is limited by the minimum distance to the obstacles $d_{\min}$. This assumption is equivalent to the idea suggested by Hunt (1985), that the obstacle blocks the turbulence scales which are larger than its size. The Eulerian length scale will be:

$$Ł_E = \min(d_{\min}, Z). \tag{25}$$

The standard deviation will be given by the relation

$$\sigma_v = \frac{L_E}{T_E} = \frac{0.6L_E}{T_L} \tag{26}$$

where T_E is the Eulerian time scale (Hanna, 1981).

Formulas (24)–(26) are only approximations for the diffusion parameters. In the general case the Lagrangian time scale, as well as velocity covariances, are tensors. However since modelling of these parameters in a built-up area is an unsolved problem and there is no preferred direction for the wind flow among the buildings, we approximate these tensors by coordinate-dependent scalars. The anisotropy of the diffusion contains contributions mainly from the average wind field. Such approximations are common in describing diffusion in a built-up area (see e.g. Eichorn (1988) and discussions in Section 5.3). The equation of motion is solved using a Monte-Carlo method. N particles' locations are derived by drawing random values from the initial source distribution. The initial particle velocities are derived from a Gaussian distribution with zero mean and standard deviation σ_v. The particles' new locations and velocities are determined using equation (21). In this way the trajectory of each particle is calculated. For a continuous source of emission rate $\dot{q}$, each particle carries pollutant of strength $\dot{q}dt/N$. The contribution of this particle to the concentration in a grid cell (i, j, k) at time t is given by

$$C_{i,j,k}(t) = \begin{cases} \dfrac{\dot{q}dt}{N\Delta X\Delta Y\Delta Z} & \text{if } i\Delta X < x(t) \leqslant (i+1)\Delta X \\ & \quad j\Delta Y < y(t) \leqslant (j+1)\Delta Y \\ & \quad k\Delta Z < z(t) \leqslant (k+1)\Delta Z \\ 0 & \text{otherwise.} \end{cases} \tag{27}$$

where $\mathbf{r}(t) = (x(t), y(t), z(t))$ is the particle's location at time t and ΔX, ΔY, ΔZ are the grid dimensions.

The total contribution up to time T is

$$C_{i,j,k} = \frac{\dot{q}dt}{N\Delta X\Delta Y\Delta Z}\sum_{n,l}\tau_l^n(i,j,k)$$

$$\tau_l^n(i,j,k) = \begin{cases} 1 & \text{if the } n\text{th particle is found in the} \\ & i,j,k \text{ cell at the } l\text{th time step} \\ 0 & \text{otherwise.} \end{cases} \tag{28}$$

5. COMPARISON TO MEASUREMENTS AND CALCULATIONS

The model described above is applied to several case studies. For all these cases there are reports in the literature either on wind tunnel measurements or on prognostic model calculations. The goal of this comparison is to evaluate the diagnostic model results against measurements or to compare its predictions to those of the prognostic models.

5.1. *A U-shape isolated building*

The diagnostic model was applied to calculate diffusion in the near field of a U-shape building (Rockle, 1994). The building height and the courtyard dimensions were 28 m. The building width was 12 m. The source was located at 2 m above the ground in the middle of the courtyard. In Fig. 4(top) we present the wind flow on a vertical cross section in the middle of the building. The bottom plot presents a horizontal cross section at the source height. In Fig. 5 isopleths of the concentration are presented on the vertical cross section in the middle of the building.

Those concentrations are normalized by $UA/\dot{q}$, where U is the wind velocity at 10 m altitude, A is the building cross section perpendicular to the wind direction and $\dot{q}$ is the source emission rate. In Fig. 6 the wind tunnel measurements are presented.

One can see that the model succeeds very well in predicting the concentration distribution. This prediction is even better than the prognostic models' calculations presented in Rockle's (1994) report.

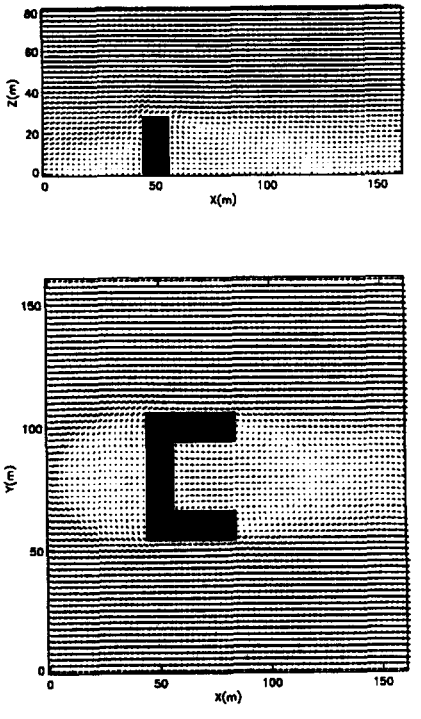

Fig. 4. The wind flow in the near field of a U-shape building: top: a cross through the middle part of the large building; bottom: top view.

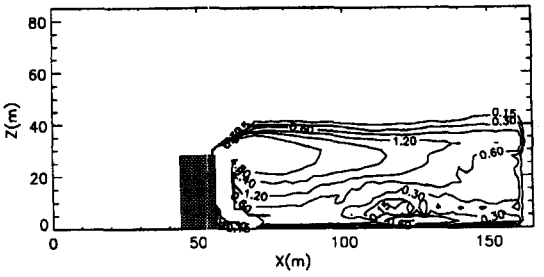

Fig. 5. Concentration contours on a vertical cross section in the middle of the building.

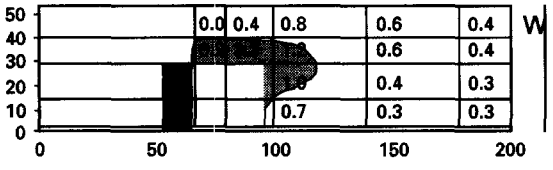

Fig. 6. Concentration distribution in the neighborhood of the U-shape building. (From Rockle (1994).) Numbers represent values obtained in wind tunnel measurements.

5.2. *Flow in the near field of two buildings*

Lee (1992) uses K–ε numerical simulation to calculate flow and dispersion around two rectangular buildings. The two buildings with dimensions 50 m $\times$ 50 m $\times$ 40 m and 50 m $\times$ 100 m $\times$ 20 m are 50 m apart. The free stream wind at 100 m altitude was 11 m s^{-1}. The source was located at the top of the higher building. The flow pattern calculated by the diagnostic model is presented in Fig. 7 and in Fig. 8 Lee's results are shown.

The downwind extension of the wake zone is a little smaller than that found in Lee's calculations. Also in our model, eddies of very light wind are developed in the space between the two buildings. In Lee's calculations the wind in this region is zero. The reason for that is that the prognostic model that uses K–ε closure, exhibits negative values for the turbulent kinetic energy and dissipation rate whenever the field gradients are large or the turbulence levels are low. In order to avoid this nonphysical behavior, Lee put zero for those variables whenever their values were negative. That is the reason that Lee's model was not able to predict the vortices between the buildings. However those vortices are responsible for accumulation of contaminant between the two buildings. In Fig. 9 we present contour maps calculated using our Lagrangian diffusion model.

Lee's results are presented in Fig. 10 for comparison.

Lee did not calculate the concentration distribution. The general behavior of the plume is similar to the qualitative description in Lee's manuscript: the plume rises up to about 75 m height and then spreads toward the ground beyond the lower building. However our model predicts penetration of the contamination into the space between the two buildings, this phenomenon not found in Lee's model. It can be

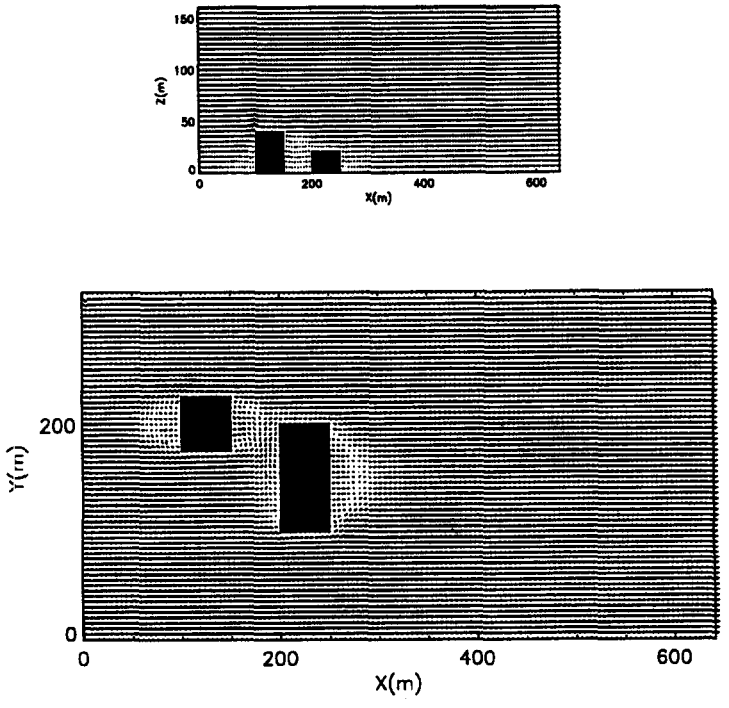

Fig. 7. The wind flow around two buildings: top: side view; bottom: top view.

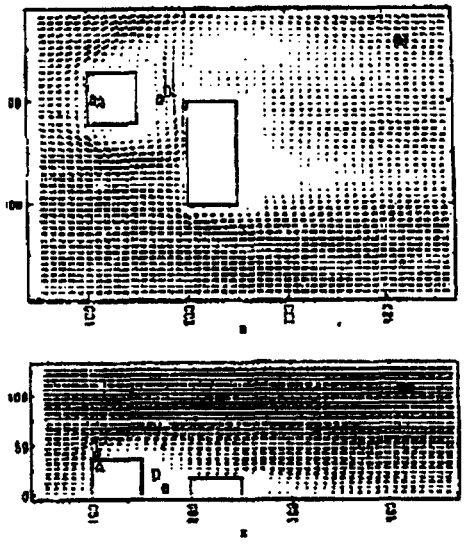

Fig. 8. The wind flow around two buildings: top: side view; bottom: top view. (From Lee (1992).)

Fig. 10. Behaviour of the concentration: top: side view; bottom: top view. (From Lee (1992).)

attributed to the small eddies which develop in this region in the diagnostic model.

5.3. *Flow in the neighborhood of a street canyon*

Dispersion on a more complicated structure is reported by Eichhorn *et al.* (1988). In this work the author solves the Navier–Stokes equations with the K-gradient approximation. K is modelled using the mixing length approximation:

$$K = l^2 |\nabla \times \mathbf{U}|. \tag{29}$$

This expression is similar to results in our Lagrangian model in the limit $t \gg T_L$.

The source is an area ground level source with emission flux rate of 1 mg s^{-1} m^{-2}. This source simulates vehicle emission at the street level. The wind velocity at 40 m altitude was 2.5 m s^{-1}. Isopleths of the concentration are presented in Fig. 11 for two cross sections: $Y = 150$ m and $Z = 2.5$ m.

The results of the diagnostic model are very similar to those of the prognostic model, both quantitatively and qualitatively (Fig. 12).

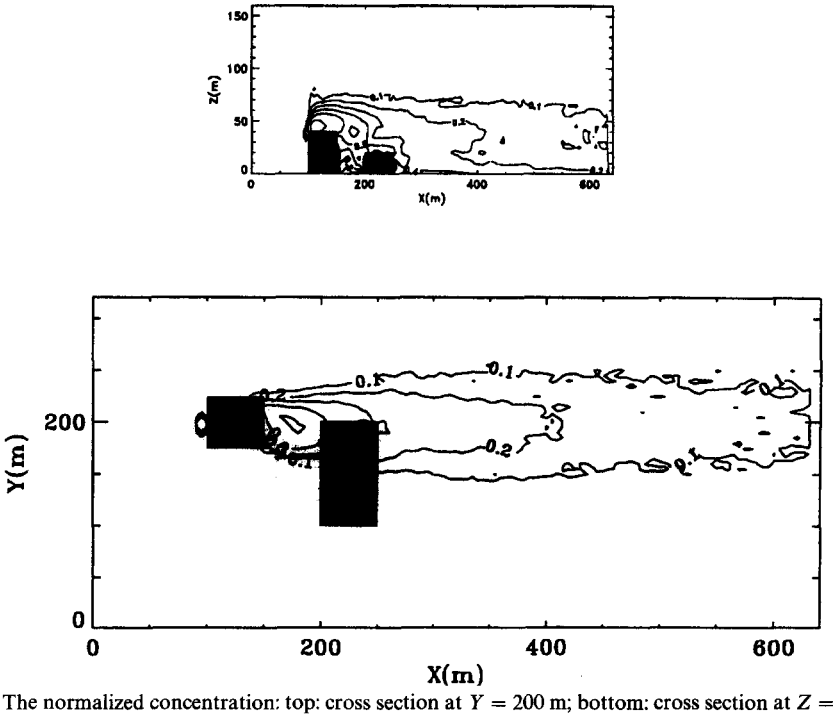

Fig. 9. The normalized concentration: top: cross section at $Y = 200$ m; bottom: cross section at $Z = 40$ m.

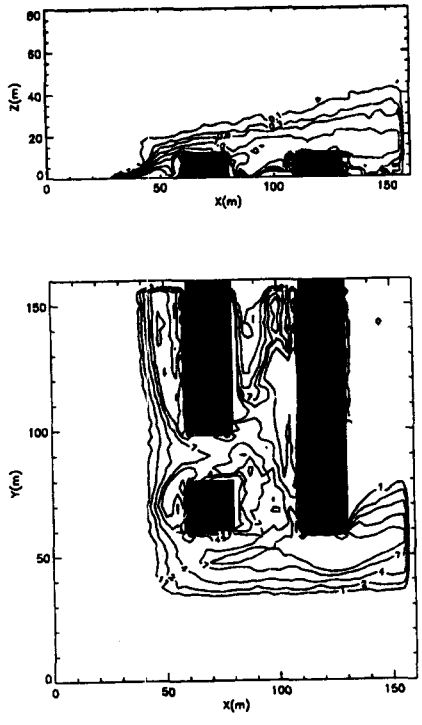

Fig. 11. The concentration isopleth (mg m^{-3}): top: cross section at $Y = 150$ m; bottom: cross section at $Z = 2.5$ m.

The differences are in the lee of the long building region. This difference is due to the fact that in Eichhorns' model the flow is affected strongly by the boundary conditions on the right side of the domain which assigns to the cavity region the free stream flow. The diagnostic model does not make this assumption and a cavity zone is developed behind the building.

5.4. *Idealized city center*

A wind tunnel experiment of diffusion with an urban canyon was performed by Cermak and Takeda (1985). The city blocks were boxes of $4h \times 4h \times h$ dimensions separated $1.5h$ from each other. h is the building height. The free stream velocity was 2 m s^{-1}. The tracer gas was released from two parallel lines located at the main street vertical to the wind direction. The concentrations on the building faces adjacent to the two continuous sources were measured. The pattern of the calculated concentrations on the walls of the street canyon are presented in Fig. 13. The concentrations are normalized by hLU/Q where U is the free stream velocity, L is the building width ($4h$) and Q is the source strength.

For comparison, Cermak's results are presented in Fig. 14.

The model was capable of predicting the phenomenon that concentrations were higher on the upwind wall of the canyon than on the downwind side. The model predicts a smaller extension of the cloud in the vertical direction on the downwind side. Therefore larger concentrations are found on this wall near the ground. However the magnitude of the concentrations found on the canyon walls are in good agreement with the measurements.

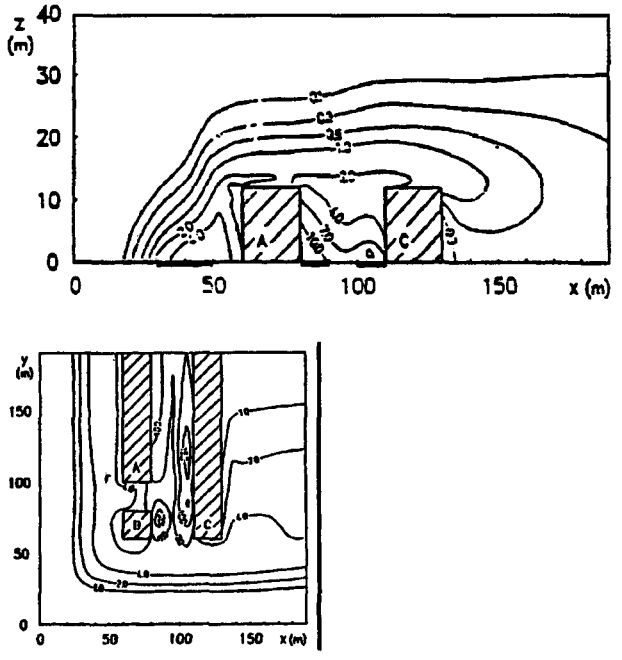

Fig. 12. The concentration isopleth (mg m^{-3}): top: cross section at $Y = 150$ m; bottom: cross section at $Z = 2.5$ m). (From Eichhorn (1988).)

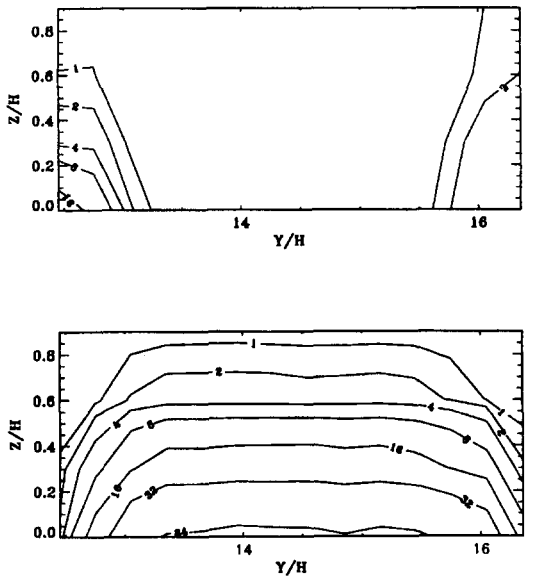

Fig. 13. The normalized concentration on the top of the canyon street. Top: downwind wall; bottom: upwind wall.

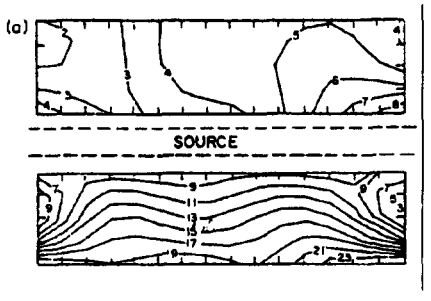

Fig. 14. The normalized concentration on the top of the canyon street. Top: downwind wall; bottom: upwind wall.

6. SUMMARY

In this manuscript we present a diagnostic model for calculating concentration distribution of a passive scalar in a built-up area. The model requires measurements of the wind velocity and direction at a reference height above the obstacles. With this measurement a diagnostic wind field is calculated using a method suggested by Rockle (1990). This field is constrained to satisfy the continuity equation. The diffusion coefficients are evaluated from this flow-field and the area structure. These coefficients are used in a Lagrangian diffusion model in an inhomogeneous field to calculate the concentration distribution given any source configuration. The model results are compared to prognostic models and wind tunnel measurements. It should be emphasized that none of the models is capable of describing wind flow accurately. The prognostic models limitations are in the closure assumptions. The success of the K-gradient closure to describe the flow field depends on the modelling of the turbulent fluxes within the built-up area. The K–ε model exhibits negative values for those fluxes whenever the field gradients are large. This occurs in the region between the buildings. The diagnostic model depends on the quality of the initial phenomenological field. The diagnostic model presented here exhibits good results in the various examples. The model is able to predict 3-D concentration distributions and to identify concentration accumulation at specific points. The model succeeds in predicting concentration distribution quantitatively and qualitatively and can be used to study many air pollution phenomena. Such phenomena are for example: stack height optimization, influence of new urban features on the pollution in its surrounding, optimization of monitoring system location, etc. The scheme of the diffusion in this manuscript describes a passive scalar. Extension to nonpassive scalar like heavy particles is a subject for further investigations.

REFERENCES

Beachlin W., Theurer W. and Plate E. J. (1992) Dispersion of gases released near ground build up areas: experimental results compared simple numerical modeling. *J. Wind Eng. Ind. Aerodynamics* **41–44,** 2721–2732.

Bowne B. E. (1974) Diffusion rates. *J. Air Poll. Control. Assoc.* **24**(9), 832–835.

Briggs G. A. (1973) Diffusion estimates for small emissions. ADTL-79 Turbulence and Diffusion Laboratory, Oak-Ridge, Tennessee.

Cermak J. E. and Takeda K. (1985) Physical modelling of urban air pollutant transport. *J. Wind Eng. Ind. Aerodynamics* **21,** 51–67.

Dinar N. (1984) Mass consistent models for wind distribution in complex terrain. Fast algorithms for three dimensional problems. *Boundary-Layer Met.* **21,** 177–199.

Eichhorn J., Schrodin R. and Zdunkowski W. (1988) Three dimensional numerical simulations of the urban climate. *Beitr. Phys. Atmos.* **61**(3), 187–203.

Gadilhe A., Janvier L. and Barnand G. (1993) Numerical and experimental modelling of the three dimensional turbulent flow through an urban square. *J. Wind Eng. Ind. Aerodynamics* **46–47,** 755–763.

Hanna S. R. (1981) Turbulence energy and Lagrangian time scale in the planetary boundary layer. In *Proc. AMS 5th Symp. on Turbulence Diffusion and Air Pollution,* Atlanta, Georgia, pp. 61–62.

Hanna S. R. and Chang J. C. (1992) Boundary-layer parametrization for applied dispersion modeling over urban areas. *Boundary-Layer Met.* **58,** 229–259.

Holzworth G. (1972) Mixing heights wind speeds and potential temperatures for urban air pollution through United States. U.S. Environ. Prof. Agency Publ. AP-101.

Hosker R. P. (1984) Flow and diffusion near obstacles. In *Atmospheric and Power Production,* SOE/TIG 27601.

Hotchkiss R. S. and Harlow F. H. (1973) Air pollution transport in street canyons. EPA-R4-73-029.

Hunt J. C. R. (1985) Turbulent diffusion from sources in complex flows. *Ann. Rev. Fluid Mech.* **17,** 447–485.

Hunter L. J., Johnson G. T. and Watson I. D. (1992) An investigation of three-dimensional characteristics of flow regimes within the urban canyon, *Atmospheric Environment* **26**(4), 425–432.

Kaplan H. and Dinar N. (1993) A three-dimensional model for calculating the concentration distribution in inhomogeneous turbulence. *Boundary-Layer Met.* **62,** 217–245.

Lee R. (1992) A finite element/finite difference approach for modelling three dimensional flow and pollutant dispersion around structures. UCRL-JC-10775 DE92 019377.

Ratto C. F. (1994) Mass-consistent models for wind fields over complex terrain: the state of the art. *Envir. Software* **9**, 247–268.

Rockle R. (1990) Bestimmung der Stomungsverhaltnisse im Bereich komplexer Bebauungsstrukturen. Ph.D. thesis, Vom Fachbereich Mechanik, der Technischen Hochschule Darmstadt, Germany.

Rockle R. (1994) Wind field and dispersion modelling in build-up areas. Lecture held at the ICTP, Trieste, Italy.

Sherman C. A. (1978) A mass-consistent model for wind fields over complex terrain. *J. appl. Met.* **17**, 312–319.

Thomson D. J. (1987) Criteria for the selection of the stochastic models of particle trajectories in turbulent flow. In *Atmospheric and Power Production*, SOE/TIG 27601.

Townsend A. A. (1956) *The Structure of Turbulent Shear Flow*. Cambridge Univ. Press, Cambridge.

Yamartino R. J. and Wiegard G. (1986) Development and evaluation of simple models for the flow, turbulence and pollutant concentration fields within an urban street canyon, *Atmospheric Environment* **20**, 2137–2156.

Zhang Y. Q., Huber A. H., Arya S. P. S. and Snyder W. H. (1993) Simulation to determine the effects of incident wind shear and turbulence level on the flow around a building. *J. Wind Eng. Ind. Aerodynamics* **46–47**, 129–134.